COMMUNICATION

CrossMark
click for updates

DNA concatamers-based biosensor for Pb(II) using electrochemical impedance spectroscopy†

Xi Zhu,[a] Huifeng Xu,*[bc] Ruolan Lin,[a] Zhonghuang Wang,[a] Bijuan Zheng,[a] Guidi Yang*[a] and Guonan Chen[c]

In this research, we demonstrate a label-free DNA concantamers-based biosensor using electrochemical impedance spectroscopy for Pb^{2+} with a 0.1 nM detection limit. This sensor was used to assay Pb^{2+} in the extraction of *Bauhinia championi*.

The detection of trace amounts of targets (DNAs, proteins, metal ions, and disease biomarkers) plays a significant role in early-stage disease diagnosis, food quality control, environmental monitoring, and homeland security. For achieving this, numerous sensing and signal amplification strategies have been developed.[1] Among them, the polymerase chain reaction (PCR) is considered to be the most successful tool[2] for the detection of DNA[3] and proteins.[4] However, PCR is limited by complicated thermal cycling steps and false positive results due to complicated thermal cycling steps.[5,6] In addition, rolling circle amplification (RCA),[7–10] and hyperbranched rolling circle amplification (HRCA)[11–14] are excellent candidates for amplifying detection due to their simplicity and high efficiency.[15,16] Although these nuclease-based amplified methods can be used for the detection of exceedingly low levels of targets, they suffer from the complexity of the experimental system due to complex operations, expensive polymerase, and tedious labels. Therefore, the development of detection without the enzyme is highly desirable.

Recently, Chen *et al.*[17,18] used two well-designed auxiliary DNA probes to hybridize with two different regions of the ssDNA by driven by the free energy of base pair without enzyme, resulting in the formation of linear DNA concatamers. This novel hybridization chain reaction (HCR) process has been used to fabricate several electrochemical biosensors by labeling different electroactive reagents on the auxiliary probes, which can be used to assay DNA,[17,18] microRNA,[19] proteins[20] and small molecules.[21]

Deoxyribozymes (DNAzyme), artificial nucleic acid enzymes, can catalyze a broad range of chemical and biological reactions in the presence of specific cofactors. These cofactors include amino acids,[22] metal ions[23] and small organic molecules.[24] Pb^{2+}, designated as an "air toxic" metal ion, is harmful to the global habitat[25,26] and ecosystem[27–29] due to its non-biodegradability. Therefore, various Pb^{2+}-dependent DNAzyme-based biosensors have been constructed, including colorimetric,[30,31] electrochemical,[32–34] fluorescence,[35–37] surface-enhanced Raman scattering,[38] and dynamic light scattering.[39] Compared with traditional methods for Pb^{2+}, such as atomic spectroscopy, these well-designed sensors avoid multiple steps of sample pretreatment, sending samples to centralized laboratories at a high cost with a long turnaround time, and a rather complex laboratory technique. Even so, the detection limits of these sensors are not satisfactory, and thus the development of a high sensitivity sensor is desired.

By combining the high selectivity of Pb^{2+}-dependent DNA-zyme and amplification of DNA concatamers, we developed an electrochemical impedance spectroscopy (EIS)-based sensor for Pb^{2+}. EIS is a useful technology for studying biomolecular interactions based on ligand binding interactions-induced change in the electrode dielectric properties.[40] To demonstrate the spectra in detail, the equivalent circuit was used to fit the EIS data. The green arrow in Fig. 1 denotes the circuit. In the impedance spectra, the semicircle portion at higher frequencies relates to the electron transfer-limited process, and the linear part at lower frequencies corresponds to diffusion. The equivalent circuit consists of the electrolyte solution resistance R_s, the surface electron transfer resistance R_{ct} which reflects the surface condition of the gold electrode surface, Warburg impedance Z_w and constant phase element related to double layer capacitance C_{dl}.[41] It is worth noting that the change in the

[a]College of Life Sciences, Fujian Agriculture and Forestry University, Fuzhou, Fujian 350002, China. E-mail: guidiyang@163.com

[b]Academy of Integrative Medicine, Fujian University of Traditional Chinese Medicine, Fuzhou, Fujian, P. R. China. E-mail: hfxu84@163.com

[c]Ministry of Education Key Laboratory of Analysis and Detection for Food Safety, Fujian Provincial Key Laboratory of Analysis and Detection for Food Safety, Department of Chemistry, Fuzhou University, Fuzhou, Fujian 350002, P. R. China
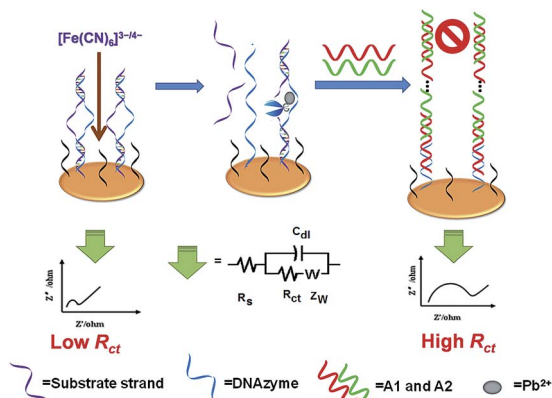
Fig. 1 Working principle of this DNA EIS-based sensor.

Fig. 2 Nyquist plots of different electrodes in a 5 mM $[Fe(CN)_6]^{3-/4-}$ solution and 0.1 M KCl. Curves a to c denote the bare electrode, DNAzyme-modified electrode, DNAzyme/substrate-modified electrode (DNA sensor), respectively; curve d and e denote the DNAzyme/substrate-modified electrode after analysis of 0.5 nM Pb^{2+} without and with HCR process, respectively.

semicircle diameter reflects the change in the interfacial charge-transfer resistance (R_{ct}), which is related to the situation on the electrode. A larger semicircle displays more resistance. Here, R_{ct} is an important parameter for quantitative detection.

The assay process contains two steps, the recognition element and the amplification element, as shown in Fig. 1. The recognition element consists of thiolated capture DNAzyme immobilized on the gold electrode surface and its substrate strand. At this stage, the negative charge of the DNA backbone on the electrode is small, resulting in a small resistance to $[Fe(CN)_6]^{3-/4-}$ probe. In the presence of Pb^{2+}, DNAzyme would catalyze the hydrolytic cleavage of the substrate strand into two pieces, resulting in only DNAzyme remaining on the electrode. The amplification element is then initiated in the presence of auxiliary A1 and A2. They are well-designed and both of them contain two fragments. The italic fragment at the 3′ end of A1 is complementary to the italic fragment of A2, and the underlined fragment at the 5′ end of A2 hybridizes with the underlined fragment of A1. Thus, the cascade of the self-assembly process between A1 and A2 forms micrometer-long DNA concatamers. In addition, the italic fragment at the 3′ end of A1 is also complementary to the italic fragment of the DNAzyme on the electrode, which helps the DNA concatamers to link to the electrode surface. During this process, the negative charge of the DNA on the electrode increases sharply, leading in a very significant resistance signal. The sequences are shown in ESI.†

For verifying the feasibility of this proposed sensor, we characterized its the preparation, recognition, and amplification. Fig. 2 indicates the R_{ct} of different modified electrodes in a 5 mmol L^{-1} $[Fe(CN)_6]^{3-/4-}$ solution with 0.1 M KCl. Compared to the bare gold electrode (curve a, $R_{ct} = 60\ \Omega$), the immobilization (curve b, $R_{ct} = 172.5\ \Omega$) and hybridization (curve c, $R_{ct} = 287\ \Omega$) of DNAzyme on the electrode leads to an increase in the negative charge and resistance, displaying larger diameters of the semicircle at higher frequencies. According to the formula in the ESI,† the surface coverage of DNAzyme on the electrode were calculated to be 1.8×10^{-12} mol cm^{-2}. After the addition of 0.5 nM Pb^{2+}, the substrate was cleaved, and the negative
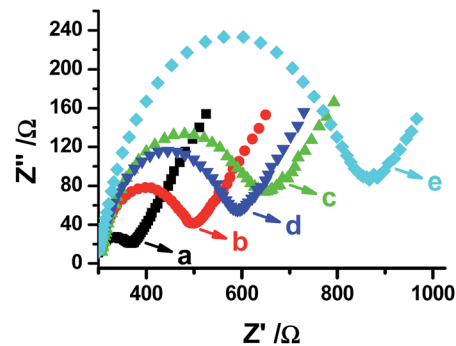
charges on the electrode surface then decreased, resulting in a slightly decreased semicircle domain (curve d, $R_{ct} = 247.5\ \Omega$). It is indicated that at 0.5 nM Pb^{2+}, about 13.8% of the cleavage efficiency of DNA enzyme was achieved. After the HCR process, the formed DNA concatamers exhibited large amounts of negative charge, resulting in a significantly increased semicircle (curve e, $R_{ct} = 441.7\ \Omega$).

To investigate the amplification of this sensor, the absolute values of the R_{ct} change ($|\Delta R_{ct}| = |R_{ct1} - R_{ct0}|$) were compared, where R_{ct0} and R_{ct1} stand for before and after the introduction of Pb^{2+}, respectively. There was a small $|\Delta R_{ct}|$ without the HCR process, while an about 4-time amplification of $|\Delta R_{ct}|$ was observed during the HCR process. These results show that this method can be used to assay trace amounts of Pb^{2+} using EIS.

Under the abovementioned optimized conditions, we investigated the impedance response of this biosensor to different Pb^{2+} concentrations. Fig. 3A and B show the impedance spectra in this system after interaction with different concentrations of Pb^{2+}. With increasing Pb^{2+} concentration, the diameter of the semicircle increased, showing that R_{ct} is proportional to Pb^{2+} concentrations. As a result, a proportional relationship was achieved between R_{ct} and the logarithm of the Pb^{2+} concentration in the range of 0.3–100 nM, as shown in the inset of Fig. 3B. The regression equation is:
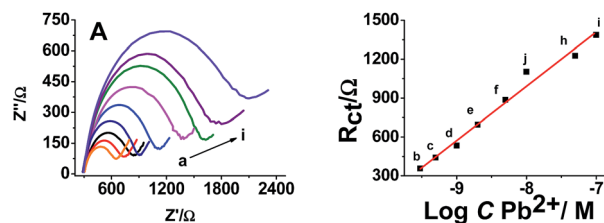

Fig. 3 (A) Impedance spectra of different Pb^{2+} concentrations: (a) 0 nM; (b) 0.3 nM; (c) 0.5 nM; (d) 1 nM; (e) 2 nM; (f) 5 nM; (g) 10 nM; (h) 50 nM; (i) 100 nM. (B) Linear relationship between R_{ct} value and the logarithm of Pb^{2+} concentration.
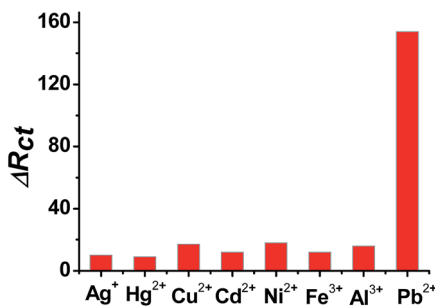
Fig. 4 Histogram of ΔR_{ct} to different metal ions, whose concentrations are 0.5 nM.

Table 1 Assay of Pb^{2+} in the extraction of a traditional Chinese herb

Sample number	Added (nM)	Found (nM)	Recover (%)
1	1.0	1.07	107
2	2.0	1.81	90.5
3	5.0	5.13	102.6
4	10.0	9.46	94.6

$$R/\Omega = 4309.68 + 414.86 \log C(Pb^{2+})\ r = 0.9910$$

where R is the R_{ct} value, $C(Pb^{2+})$ is Pb^{2+} concentration, and r is the regression coefficient. The detection limit was calculated to be 0.1 nM based on the 3σ per slope (σ is the standard deviation of blank sample for 10 times), which is prior to those of DNA-zyme-based electrochemical biosensors.[32,33,42]

Good specificity is one of the most important parameters for a sensor. Here, we performed a comparison experiment on non-target metal ions and target Pb^{2+}. The non-target metal ions included Ag^{+}, Hg^{2+}, Cu^{2+}, Cd^{2+}, Ni^{2+}, Fe^{3+}, and Al^{3+}. The concentrations of these non-target metal ions and Pb^{2+} were 0.5 nM. The experimental results are shown in Fig. S1.† ΔR_{ct} represents the R_{ct} change, that is, $\Delta R_{ct} = R_{ct1} - R_{ct0}$, where R_{ct0} and R_{ct1} stand for before and after the introduction of Pb^{2+} during the HCR process, respectively. It is clear that for non-target metal ions, there are small ΔR_{ct} values. On the contrary, an obvious ΔR_{ct} was observed in the presence of Pb^{2+}. This result confirms that this proposed method has excellent selectivity to Pb^{2+} due to high selectivity of DNAzyme (Fig. 4).

This biosensor was also applied to assay Pb^{2+} in the extraction of *Bauhinia championi*, a traditional Chinese herb for relieving osteoarthritis.[43] The detection results are shown in Table 1. Satisfactory recoveries (90.5–107%) were obtained, suggesting that this method can provide an efficient tool for the detection of Pb^{2+} in the traditional Chinese herb.

In summary, by combining the amplification of the HCR process and Pb^{2+}-dependent DNAzyme, we constructed an EIS-based DNA sensor for Pb^{2+} with a detection limit of 0.1 nM. Further, it was used for the detection of river samples. It showed promise for the detection of metal ions in the traditional Chinese herb.

Notes and references

1 Y. F. Wu, W. Wei and S. Q. Liu, *Acc. Chem. Res.*, 2012, **45**, 1441–1450.
2 D. Rodriguez-Lazaro, M. Hernandez, M. Scortti, T. Esteve, J. A. Va zquez-Boland and M. Pla, *Appl. Environ. Microbiol.*, 2004, **70**, 1366–1377.
3 S. Y. Liu, J. A. Metcalf, J. W. Mellors and J. M. Coffin, *J. Clin. Microbiol.*, 2003, **41**, 4531–4536.
4 H. Q. Zhang, Q. Zhao, X. F. Li and X. C. Le, *Analyst*, 2007, **132**, 724–737.
5 G. Nallur, C. Luo, L. Fang, S. Cooley, V. Dave, J. Lambert, K. Kukanskis, S. Kingsmore, R. Lasken and B. Schweitzer, *Nucleic Acids Res.*, 2001, **29**(23), e118.
6 F. Li, C. Zhao, W. Zhang, S. Cui, J. Meng, J. Wu and D. Y. Zhang, *J. Clin. Microbiol.*, 2005, **43**, 6086–6090.
7 B. Schweitzer, S. Roberts, B. Grimwade, W. Shao, M. Wang, Q. Fu, Q. Shu, I. Laroche, Z. Zhou, V. T. Tchernev, J. Christiansen, M. Velleca and S. F. Kingsmore, *Nat. Biotechnol.*, 2002, **20**, 359.
8 N. O. Fischer, T. M. Tarasow and J. B. Tok, *Anal. Biochem.*, 2008, **373**, 121–128.
9 D. A. Di Giusto, W. A. Wlassoff, J. J. Gooding, B. A. Messerle and G. C. King, *Nucleic Acids Res.*, 2005, **33**, e64.
10 N. Li, J. Li and W. Zhong, *Electrophoresis*, 2007, **29**, 424.
11 S. Kaocharoen, B. Wang, K. M. Tsui, F. Trilles, F. Kong and W. Meyer, *Electrophoresis*, 2008, **29**, 3183–3191.
12 B. Wang, S. J. Potter, Y. Lin, A. L. Cunningham, D. E. Dwyer, Y. Su, X. Ma, Y. Hou and N. K. Saksena, *J. Clin. Microbiol.*, 2005, **43**, 2339–2344.
13 Y. Q. Cheng, X. Zhang, Z. P. Li, X. X. Jiao and Y. C. Wang, *Angew. Chem., Int. Ed.*, 2009, **48**, 3268–3272.
14 A. P. Cao and C. Y. Zhang, *Anal. Chem.*, 2012, **84**, 6199–6205.
15 W. Cheng, F. Yan, L. Ding, H. Ju and Y. Yin, *Anal. Chem.*, 2010, **82**, 3337–3342.
16 Q. Su, D. Xing and X. M. Zhou, *Biosens. Bioelectron.*, 2010, **25**, 1615–1621.
17 X. Chen, Y.-H. Lin, J. Li, L.-S. Lin, G.-N. Chen and H.-H. Yang, *Chem. Commun.*, 2011, **47**, 12116–12118.
18 X. Chen, C.-Y. Hong, Y.-H. Lin, J.-H. Chen, G.-N. Chen and H.-H. Yang, *Anal. Chem.*, 2012, **84**, 8277–8283.
19 C.-Y. Hong, X. Chen, T. Liu, J. Li, H.-H. Yang, J.-H. Chen and G.-N. Chen, *Biosens. Bioelectron.*, 2013, **50**, 132–136.
20 L. P. Jiang, J. D. Peng, R. Yuan, Y. Q. Chai, Y. L. Yuan, L. J. Bai and Y. Wang, *Analyst*, 2013, **138**, 4818.
21 B. Q. Liu, B. Zhang, G. N. Chen, H. H. Yang and D. P. Tang, *Biosens. Bioelectron.*, 2014, **53**, 390–398.

22 E. Vianini, M. Palumbo and B. Gatto, *Bioorg. Med. Chem.*, 2001, **9**, 2543–2548.

23 N. Carmi, H. R. Balkhi and R. R. Breaker, *Proc. Natl. Acad. Sci. U. S. A.*, 1998, **95**, 2233–2237.

24 D. E. Huizenga and J. W. Szostak, *Biochemistry*, 1995, **34**, 656.

25 C. Winder, N. G. Carmichael and P. D. Lewis, *Trends Neurosci.*, 1982, **5**, 207–209.

26 S. Araki, H. Sato, K. Yokoyama and K. Murata, *Am. J. Ind. Med.*, 2000, **37**, 193–204.

27 Environmental Protection Agency, *Control of Emissions of Hazardous Air Pollutants from Motor Vehicles and Motor Vehicle Fuels*, EPA-420/R-00-023, Washington, DC, 2000.

28 R. S. Shetty, S. K. Deo, P. Shah, Y. Sun, B. P. Rosen and S. Daunert, *Anal. Bioanal. Chem.*, 2003, **376**, 11–17.

29 D. A. Blake, R. M. Jones, R. C. Blake, A. R. Pavlov, I. A. Darwish and H. Yu, *Biosens. Bioelectron.*, 2001, **16**, 799–809.

30 X. Zhu, X. Y. Gao, Q. D. Liu, Z. Y. Lin, B. Qiu and G. N. Chen, *Chem. Commun.*, 2011, **47**, 7437–7439.

31 D. Mazumdar, J. Liu, G. Lu, J. Zhou and Y. Lu, *Chem. Commun.*, 2010, **46**, 1416–1418.

32 Y. Xiao, A. Rowe and K. Plaxco, *J. Am. Chem. Soc.*, 2007, **129**, 262–263.

33 L. Shen, Z. Chen, Y. Li, S. He, S. Xie, X. Xu, Z. Liang, X. Meng, Q. Li, Z. Zhu, M. Li, X. C. Le and Y. Shao, *Anal. Chem.*, 2008, 6323–6328.

34 R. M. Kong, Z. L. Song, H. M. Meng, X. B. Zhang, G. L. Shen and R. Q. Yu, *Biosens. Bioelectron.*, 2014, **54**, 442–447.

35 H. Xu, P. Xu, S. Gao, S. Zhang, X. Zhao, C. Fan and X. Zuo, *Biosens. Bioelectron.*, 2013, **43**, 520–523.

36 Y. Xiang, A. Tong and Y. Lu, *J. Am. Chem. Soc.*, 2009, **131**, 15352–15357.

37 L. Zhang, B. Han, T. Li and E. Wang, *Chem. Commun.*, 2011, **47**, 3099–3101.

38 Y. Wang and J. Irudayaraj, *Chem. Commun.*, 2011, **47**, 4394–4396.

39 X. Miao, L. Ling and X. Shuai, *Chem. Commun.*, 2011, **47**, 4192–4194.

40 E. Katz and I. Willner, *Electroanalysis*, 2003, **15**, 913.

41 F. Patolsky, A. Lichtenstein and I. Willner, *J. Am. Chem. Soc.*, 2001, **123**, 5194–5205.

42 Q. Fan, J. Zhao, H. Li, L. Zhu and G. Li, *Biosens. Bioelectron.*, 2012, **33**, 211–215.

43 H. T. Li, X. H. Li, G. Z. Liu, J. S. Chen, X. P. Weng, F. Y. Liu, H. F. Xu, X. X. Liu and H. Z. Ye, *Int. J. Mol. Med.*, 2013, **32**, 1329–1336.